Vol. 18, No. 3 (2019) 1179-1187
Revista Mexicana de Ingeniería Química

SPHEROIDAL ZINC OXIDE NANOPARTICLES SYNTHESIZED BY SEMICONTINUOUS PRECIPITATION METHOD AT LOW TEMPERATURES

NANOPARTÍCULAS ESFÉRICAS DE ÓXIDO DE ZINC SINTETIZADAS POR UN MÉTODO DE PRECIPITACIÓN SEMICONTINUA A BAJAS TEMPERATURAS

S. López-Cuenca[1], J. Aguilar-Martínez[2], M. Rabelero-Velasco[3], F.J. Hernández-Ibarra[4], L.C. López-Ureta[1], M.A. Pedroza-Toscano[5]*

[1]*Departamento de investigación, Instituto Tecnológico José Mario Molina Pasquel y Henríquez Campus Zapopan. Zapopan Jalisco, C. P. 45019, Mexico.*

[2]*Departamento de ciencias tecnologicas. Centro Universitario de la Ciénega, Universidad de Guadalajara. Ocotlan Jalisco, C. P. 47820, Mexico.*

[3]*Departamento de Ingeniería Química. CUCEI, Universidad de Guadalajara. Guadalajara Jalisco, C.P. 44430, Mexico*

[4]*Departamento de investigación, Instituto Tecnologico Jose Mario Molina Pasquel y Henriquez Campus Tequila. Tequila Jalisco,C.P. 46400, Mexico*

[5]*Departamento de investigación, Centro Universitario UTEG. Plantel Olímpica. Guadalajara Jalisco, C. P. 44430, Mexico.*

Received: October 1, 2018; Accepted: October 21, 2018

Abstract

The synthesis of spheroidal high purity zinc oxide (ZnO) and crystal size in a range of 20 and 45 nm, using the semicontinuous precipitation method is reported in this work. The ZnO nanoparticles (ZnO-NPs) were made by hydrolysis of $Zn(NO_3)_2$ with NaOH aqueous solution and precipitation at temperatures below 90 °C. The ultrafine powder of ZnO was analyzed by X-ray diffraction (XRD), where the formation of ZnO nanoparticles and hexagonal crystal structure (wurtzite) was corroborated. Spheroidal nanoparticles were observed by transmission electron microscopy (TEM) and energy dispersive aX-ray (EDX) spectra confirming the presence of high purity ZnO-NPs. A factorial experimental model 2^3 was performed to grant statistical validity of the experimental procedure. The antibacterial activity of ZnO-NPs was tested by the agar disk diffusion method, against *S. aureus* and *E. coli*.

Keywords: ZnO nanoparticles, static analysis, precipitation, antibacterial.

Resumen

En este trabajo se reporta la síntesis de nanopartículas esferoidales de óxido de zinc (ZnO), obtenidas por precipitación semicontinua con tamaño de cristal en el rango de 20 y 45 nm. Las nanopartículas de ZnO (ZnO-NPs) se obtuvieron mediante hidrólisis de $Zn(NO_3)_2$ con solución de NaOH y precipitadas a temperaturas inferiores a 90 °C. El polvo ultrafino obtenido de ZnO, fue analizado por difracción de rayos X (XRD), donde se corroboró la formación de ZnO-NPs con una estructura hexagonal (wurtzita). Se pudieron observar nanopartículas esferoidales por microscopía electrónica de transmisión (TEM) y, mediante energía de dispersión de rayos X (EDS), también se confirmó la alta pureza de las ZnO-NPs. Así mismo, se realizó un diseño factorial 2^3 para validar estadísticamente el procedimiento experimental y, se probó la actividad antibacterial de ZnO-NPs por el método de difusión en agar para las bacterias *S. aureus* y *E. coli*.

Palabras clave: Nanopartículas de ZnO, análisis estadístico, precipitación, antibacterial.

1 Introduction

Perhaps, ZnO is one of the most studied materials, because it presents high versatility in applications at low cost. This material is used in the production of lasers (Zhang *et al*., 2009), sensors (Lupan *et al*., 2014; Kalyamwar *et al*., 2013), photovoltaic cells (Gosh *et al*., 2013; Flickyngerová *et al*., 2010), antimicrobials (Gosh *et al*., 2015), piezoelectric materials (Reshak *et al*., 2014; Gullapalli *et al*., 2010), nanofiltration membranes (Pérez - Sicairos *et al*., 2016) and it is part of nanostructured materials such as nanorods (Devaraj *et al*., 2013), and nanospheres (Onwudiwe *et al*., 2015), where physical-chemical properties change according to the structure type and particle size.

* *Corresponding author. E-mail*: mpedroza@uteg.edu.mx

issn-e: 2395-8472

Several methods have been used to prepare ZnO nanostructures. Among them, we can mention spray pyrolysis (Filali *et al*., 2015), microemulsions either inverse or bicontinuous (Sharma *et al*., 2014; Jen-Chieh *et al*., 2012; Hingorani *et al*., 1993), sol-gel process (Wasan *et al*., 2012), chemical precipitation (Ovando-Medina *et al*., 2018; Pookmanee *et al*., 2010; Swaroop *et al*., 2015), hydrothermal (Shim *et al*., 2011; Xia Kong *et al*., 2017), polymeric precursor (Pechini) (Devaraj *et al*., 2013), sonochemical (Geng *et al*., 2012) and solochemical (Gusatti *et al*., 2010; Gusatti *et al*., 2011; Gusatti *et al*., 2013; Sornalatha *et al*., 2015). The most used colloidal methods to synthesize ZnO-NPs with controlled size has been by inverse microemulsion, obtaining particle size less than 10 nm, but with the drawback of low yield, and bicontinuous microemulsion. This last one with high yield but bigger nanoparticles (Romo *et al*., 2011; Hingorani *et al*., 1993; Lim *et al*., 1998).

The chemical precipitation method presents some advantages because it is not necessary addition of organic solvents or surfactant agents. Moreover, calcination of precipitates is not required. Furthermore, it is possible to prepare different structures, that depends on temperature and both; type and concentration of the precursor agent. Nanorods of ZnO were synthesized by Gusatti *et al*. (2013), they used $ZnCl_2$ as precursor, temperatures of 50, 70 y 90 ºC and concentrations of 0.3 and 0.5 mol/L of $ZnCl_2$. The temperatures of 50 and 70 ºC had influence on particle size, however, at temperatures of 90 ºC and 0.5 mol/L, the particle size did not increase. This behavior was attributed to the formation of $Zn(OH)_2$ clusters induced by high temperatures (90 ºC). On the other hand, Shymaa S. A. and Asmaa S. (2014), perform synthesis of nanorods at two temperatures: 70 and 80 ºC, using zinc nitrate hexahydrate as a precursor agent. There are several methods to synthesize different ZnO structures that depend of precursor agent. Zinc nitrate hexahydrate and zinc acetate dehydrate were used to synthesize cauliflower-like nanoflower ZnO nanostructures, respectively. Spherical and hexagonal structures were prepared, by using different precipitant agent and concentrations (Sornalatha *et al*., 2015).

In this work, we report the synthesis of ZnO-NPs at low temperatures using the semicontinuous precipitation method and the influence of the variables involved in the particles size, such as, precursor agent concentration, temperature and addition time of precipitant agent. By this method, we obtained high yield inorganic nanoparticles in a better sustainable way. The inferences were based on statistics methods. ZnO-NPs were observed by transmission electron microscopy (TEM) and characterized by X-ray diffraction (XRD).

2 Materials and methods

Zinc nitrate hexahydrate $Zn(NO_3)_2{\cdot}6H_2O$ 98% pure (Sigma-Aldrich) and sodium hydroxide NaOH, 98.2% pure (Golden Bell), were used as received. De-ionized and triple-distilled water with conductivity smaller than 6 μS/cm was used.

2.1 Experimental design

The different combination of three variable was explored in a factorial experimental model 2^3, i.e., $Zn(NO_3)_2{\cdot}6H_2O$ molar concentration, reaction time and temperature. Two levels for each parameter was tested. For concentrations as precursor agent of the ZnO-NPs, the levels were 0.1 and 0.5 M, for the reaction temperature were 65 and 80 °C and for the time were 60 and 90 minutes. Table 1 shows the complete formulations. The statistical analysis was performed by Statgraphics (Warrenton, VA).

2.2 Precipitation of ZnO-NPs

The precipitation reaction was carried out in duplicate, using a 250 mL jacketed glass reactor. The reactor had an inlet for feeding of the NaOH aqueous solution. The procedure reaction started with loading the zinc nitrate aqueous solution (75 mL) into the reactor, and the temperature was carried out, either 65 or 80 °C. Then, the stoichiometric quantity of NaOH aqueous solution 1 M was added semicontinuously using a syringe, at one-minute intervals, by either 60 min or 90 min according to Table 1. Finished the addition of the precipitated agent, the system was allowed proceed for 30 minutes more, keeping temperature and agitation. Nanoparticles of ZnO obtained were washed by mixing it with a water-acetone solution (81/19, w/w) at room temperature, and placed into an ultrasonic bath to remove unreacted materials. The resulting mixture was then centrifuged at 9500 rpm to separate solids. This procedure was followed several times to obtain the most purified ZnO-NPs. Finally, purified materials were dried in an oven at 60 °C for 24 hours.

2.3 ZnO-NPs characterization

The presence and purity of ZnO-NPs in the ultrafine powder obtained at the end of purification procedure, was determined by energy dispersive X-ray spectroscopy coupled to a scanning electron microscopy (SEM-EDS) from Tescan, model MIRA 3 LMU-Bruker. The structure and size of ZnO-NPs were obtained by XRD in an Empyrean diffractometer from PANalytical. ZnO purified powders were scanned in the range of 10 to 90, 2θ degrees, by which the diffraction patterns of the ZnO-NPs were obtained. Morphology of ZnO-NPs was confirmed by TEM in a JEOL-1010 apparatus. The ZnO purified powder was re-dispersed in distilled water and a drop of dispersion was deposited on a copper grid, allowing evaporate the solvent at room temperature. The particle average crystal sizes were obtained by using the Scherrer equation:

$$d = \frac{K\lambda}{\beta \cos\theta} \quad (1)$$

being d the mean diameter of the nanoparticles, in nm, K the dimensional factor (0.9), λ the X-ray wavelength (0.154 nm), β the line broadening at half the maximum intensity in radians, and θ the Bragg's angle.

2.4 Antibacterial activity of zinc oxide nanoparticles

The ZnO-NPs synthesized was tested for antibacterial activity by agar disk diffusion method against the Gram positive pathogenic bacteria *Staphylococcus aureus* (ATCC 25923) and Gram negative *Escherichia coli* (ATCC 25922). Briefly, after the pure cultures of bacteria were subcultured on nutrient broth, 0.15 mL (approximately 10^7 CFU/mL) of a bacterial suspension of a 0.5 McFarland standard inoculum of each strain was spread homogeneously onto the individual agar plates using sterile cotton swabs. Sterile filter paper disc (6 mm diameter) impregnated by three different ZnO-NPs concentration (1, 2, 3 mg/disc), were placed on the nutrient agar plates on which bacteria were spread. The resulting growth of bacteria was observed after 24 h of incubating the plates a 37 °C, the presence of inhibition zones was measured. For each bacterial strain, three replications were performed.

Determination of minimum inhibitory concentration (MIC) of ZnO-NPs. MIC is defined as the lowest concentration of the antimicrobial agent that inhibits the growth of microorganism after 24 hours of incubation (Mostafa *et al*., 2015). The ZnO-NPs were used to determine its minimal inhibitory concentration (MIC) to evaluate its efficiency in controlling pathogenic bacteria (*S. aureus* and *E. coli*).

3 Results and discussion

Nanoparticles of zinc oxide were synthesized by the conditions described above. During the reaction process, at the beginning of the addition of NaOH, the clear solution changed slightly to whitish, which is indicative of the formation of zinc oxide nanoparticles. Throughout the reaction time, stable solutions were observed, that is, they did not show coalescence. The formation of zinc oxide nanoparticles starts from the Zn^{2+} ions from the Zn precursor agent, which react with OH^- ions from the NaOH, producing complexes $Zn(OH)_4^{-2}$, which when reaching the saturation point they decompose in nuclei ZnO (Shymaa *et al*., 2014), and from there, the process of growth of the ZnO NPs begins.

Through statistical analysis (discussed below), only statistically validates the variables that influence the crystal size. This analysis shows that the variable that has the most influence statistically is the concentration of the precursor agent on the response variable that is crystal size measured through the Scherrer equation.

3.1 EDS analysis

After purification process, the collected ultrafine powders were first analyzed by SEM-EDS to verify the ZnO presence and purity from it. The EDS spectrum is shown in Fig. 1, where an intense signal at 1 and 8.7 keV by the presence of ZnO is observed.

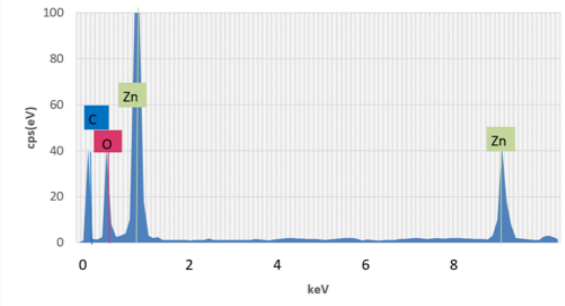

Fig. 1. EDS spectra of zinc oxide nanoparticles.

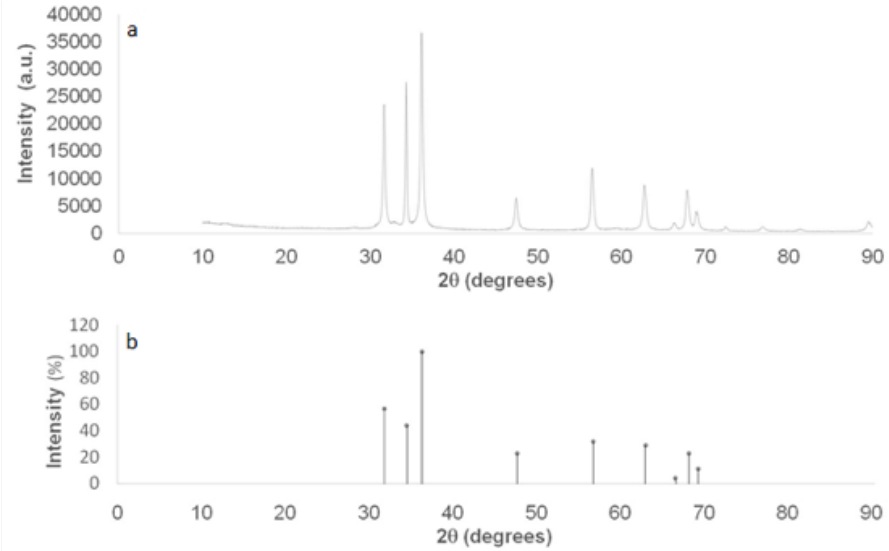

Fig. 2. XRD pattern of ZnO. a) Powder synthesized at 80 °C. b) ICDD No. 36-1451.

3.2 X-Ray diffraction pattern

Fig. 2 (a) shows the XRD pattern diffraction of ZnO powder for the sample synthesized at 80 °C, with the dosage time of 60 minutes and $Zn(NO_3)_2{\cdot}6H_2O$, 0.1 M (experiment 6 in Table 1). XRD pattern of the precipitate shows ZnO material with hexagonal wurtzite structure (36-1451, Fig. 2 (b)), as shown by Gusatti *et al*. (2011). All diffraction peaks show small deviations from the 2θ angles of: 32°, 34°, 36°, 48°, 57°, 63°, 66° and 68°, that correspond to the crystalline planes: (100), (002), (101), (102), (110), (103), (200) and (112).

The deviations in 2θ angles are attributed to the fact that the structure of ZnO nanoparticles are not perfect crystals, but rather they present small irregularities. Similar XRD patterns were obtained for all samples. These results confirm that ZnO-NPs were formed with low size and high purity (no other crystalline planes were found). Table 2 shows the crystal size estimated with Scherrer equation calculated with the (101) plane and the percent yield calculated by gravimetric analysis, where stand outs the crystal size increase since 23 nm to 31 nm and reaction performance above 90%.

According to Table 2 in conjunction with the statistical analysis, it is observed that the higher the concentration, the smaller the particle diameter, that is, the crystal size for the samples made with a concentration of 0.1 M are greater than for those made with concentration of 0.5 M, this due to the Zn^{2+}/OH^- ratio (Gusatti *et al*., 2013), since the higher the ratio as in the case of the 0.5 M concentration, the creation of nucleation centers is favored, decreasing the aggregation speed due to the high competition between them and the low availability of Zn^{2+} ions resulting in slow growth and small sizes, in the case of the concentration of 0.1 M the ratio Zn^{2+}/OH^- is lower, when adding the NaOH solution semicontinuously, few nucleation centers are created that grow rapidly interacting with the high availability of surrounding Zn^{2+} ions, so the rate of aggregation is greater creating larger crystals. It is also observed that there is no significant difference between the crystal size with respect to the temperature of 65 °C and 80 °C, since the average diameters are very similar.

Table 1. Factors and levels considered on the experimental design.

Experiment	Concentration (M)	Time (min)	Temperature (ºC)
1	0.1	60	65
2	0.1	60	80
3	0.1	90	65
4	0.1	90	80
5	0.5	60	65
6	0.5	60	80
7	0.5	90	65
8	0.5	90	80

For the reaction time of 60 min and 90 min, we can infer that it has a slight influence on the crystal size, that is, when changing from 60 min to 90 min of reaction time, there is an increase of around 2 nm in the size of the crystal, although it was expected that the crystal size would be smaller when increasing the reaction time, since the ratio of Zn^{2+}/OH^{-} is increased. This is disadvantaged by the fact that there is greater interaction between the same nanoparticles and ions Zn^{2+} available for a longer time, thus increasing its size and decreasing the effect of the Zn^{2+}/OH^{-} ratio.

3.3 Transmission electron microscopy analysis

ZnO-NPs structure was observed and analyzed by TEM. Fig. 3 shows a micrograph of purified powder from the synthesized sample in experiment 5 (Table 1). Nanoparticles of different size (similar of that obtained from Scherrer equation) with irregular hexagonal structure (similar to XRD pattern) can be appreciated, but some of them are agglomerated as reported Gusatti *et al*., 2011. Similar micrographs ware obtained for all the samples, with a size distribution between 20 and 45 nm, this agrees whit the size of the crystal estimated with Scherrer equation; Table 2 shows the average diameters for all the samples. This type of structure is attributed to the form of synthesis performed; since, in other reports in the literature (Gusatti *et al*., 2013; Shymaa *et al*., 2014; Sornalatha *et al*., 2015), for similar conditions of concentration and temperature of 50 ºC and 70 ºC, but adding the precursor agent of ZnO slowly over the NaOH solution, nanorods are obtained.

Table 2. Crystal size estimated with Scherrer equation and Dn determined by TEM.

Experiment	Crystal Size Scherrer equation (nm)	Diameter (nm) TEM	Yield (%)
1	27	34.2	93.1
2	27.9	33.4	92.2
3	31.3	35.8	94.5
4	26.7	32.6	91.2
5	25.7	32.1	90.4
6	23.5	28.4	89.9
7	26.7	29.5	87.7
8	27.8	33.2	91.2

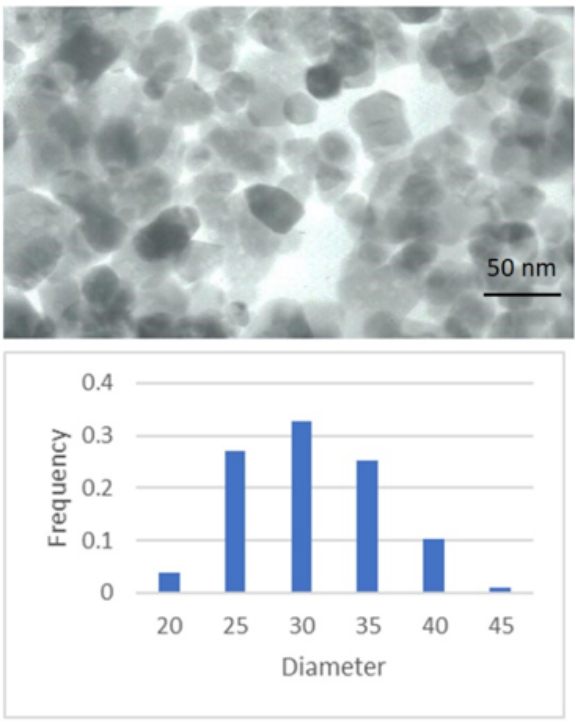

Fig. 3. TEM micrograph and their histogram of sample obtained at 65 °C, 60 minutes of reaction time and 0.5 M of zinc nitrate.

This due to that there is a low ratio of Zn^{2+}/OH^{-} (high pH) that favors the growth of the particles until developing in nanorods, since there are few nucleation centers with high availability of Zn^{2+} ions (Gusatti *et al*., 2013). Spheroidal structures are also reported when the reaction temperature increases to 90 ºC (Gusatti *et al*., 2013). In our case, the structure obtained for all our samples is spheroidal type obtained at temperatures below 90 ºC. This morphological structure is attributed to the preparation method, and the agent that was added was NaOH in a semicontinuous manner, so that the Zn^{2+}/OH^{-} ratio is high (low pH) which allows to create many nucleation centers that grow slowly as there is availability of OH^{-} groups. When adding NaOH, at the same time these OH^{-} groups react quickly, allowing the pH to be maintained low throughout the reaction.

3.4 Statistical approach

The effect of the three variables, concentration (A), time reaction (B) and temperature (C), assuming that these influences the crystal size of ZnO synthesized, this last one as response variable, was tested in an analysis of variance (ANOVA) study with a 2^3 factorial design.

Table 3. Analysis of variance (ANOVA) from the different variables studied.

Source	Sum of Squares	Df	MEan Square	F-Ratio	P-value
A:Concentration	25.6936	1	25.6936	5.73	0.0436
B:Time	14.005	1	14.005	3.12	0.1151
C:Temperature	3.5865	1	3.5865	0.8	0.3972
AB	0.36012	1	0.36012	0.08	0.7841
AC	3.10053	1	3.10053	0.69	0.4298
BC	0.317175	1	0.317175	0.07	0.797
Blocks	2.85435	1	2.85435	0.64	0.448
Total error	35.8674	8	4.48343		
Total (corr.)	85.7847	15			

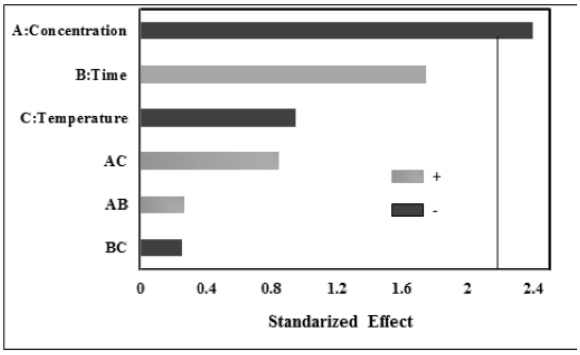

Fig. 4. Standardized pareto chart for crystal size.

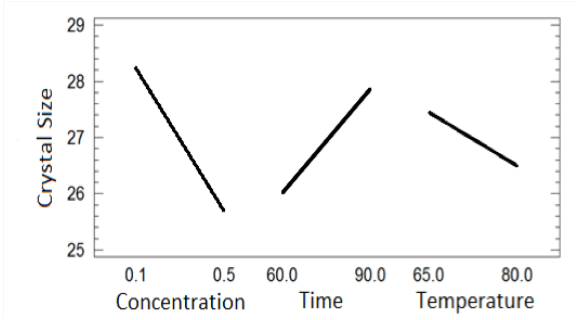

Fig. 5. Effect of concentration, time and temperature on crystal size.

One advantage of the method is that this also regards the interactions between these variables on the response. These are called AB, AC, and BC as the concentration-time interaction, concentration-temperature interaction and the time-temperature one, respectively. The statistical procedures were performed according to the most consulted and referenced theory and literature (Montgomery, 2017). On this way, a p-value for each factor below 0.05 indicates 95% of statistical significance of cause and effect evidence. The results obtained from the analysis of variance (ANOVA) are shown in Table 3. It shows the sum of squares, freedom degrees (Df), squares mean, F-Ratio and P-Value. It is observed that the only P-value less than 0.05 is for the concentration, with 95% confidence it can be said, that is the only variable that has an influence over the crystal size of ZnO-NPs, meanwhile the others variables, reaction time and temperature, have not statistical significance in their correlation with size.

Because ANOVA only predicts the factors that affect significantly the crystal size but not the way in which they do it, is necessary to describe how each factor acts to understand the corresponding correlations. Fig. 5 shows the main effects produced for the variables: concentration, time and temperature over the crystal size, where we can observe that when we increase the concentration of the precursor solution, the crystal size decreases. The same effect is observed when the temperature increases. However, when the reaction time is longer, the size of the crystal grows. On the other hand, although other authors have reported similar results with respect to crystal size (Gusatti *et al*., 2013; Shymaa *et al*., 2014; Sornalatha *et al*., 2015), correlation with time and correlation temperature are not enough significant in their statistics, so such factors have a very poor influence on the size of the crystals. An increase the concentration of the precursor solution, a decreasing in crystal size is produced.

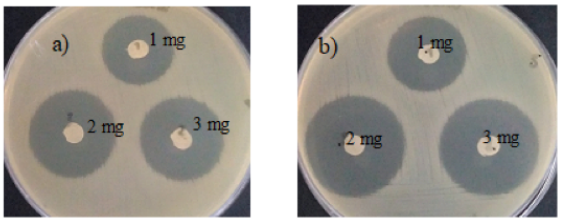

Fig. 6. Inhibition zone for a) *E. coli* b) *S. aureus*.

3.5 Antibacterial activity of zinc oxide nanoparticles

The result revealed that ZnO-NPs has antibacterial activity against both tested bacterial strains. The nanoparticles exhibited maximum inhibition zone for 3 mg/disk of 12.8 mm and 15.8 mm for *E. coli* and *S. aureus* respectively. This is consistent with previously reported results (Ibrahem *et al*., 2017). Fig. 6 shows the zones of inhibition for sample 5 (all the samples exhibit similar inhibition zone). The minimum inhibitory concentration (MIC) of zinc oxide nanoparticles was evaluated. The results showed that the MIC of ZnO-NPs against *S. aureus* and *E. coli* was less than 0.15 mg/disk.

Conclusions

Spheroidal ZnO-NPs with hexagonal structure were obtained by precipitation method at low temperatures when the sodium hydroxide solution was added semicontinuously to the zinc nitrate solution. The characterizations carried out by XRD, TEM and EDS demonstrated the obtaining of spheroidal ZnO-NPs synthesized at a temperature lower than 90 °C. The semicontinuous precipitation method resulted to be an easy and environment friendly process to synthesize ZnO nanoparticles from 20 to 45 nm with high purity and with hexagonal wurtzite irregular structure. The ANOVA analysis report a good correlation between precursor solution concentration and particles size with a statistical significance higher than 95 percent, allowing identify in this study, that the size of the particles reduces as the zinc nitrate concentration increase. Both bacteria, *S. aureus* and *E. coli*, were inhibited by ZnO-NPs. However, *S. aureus* was more susceptible than *E. coli*.

Acknowledgements

The support of TecNM given to this project are gratefully acknowledged. The many helpful discussions with Rodolfo Salazar-Peña, professor of Centro Universitario UTEG, Mexico, about the statistical analysis are gratefully acknowledged.

References

Devaraj, R., Karthikeyan, K. and Jeyasubramanian, K. (2013). Synthesis and properties of ZnO nanorods by modified Pechini process. *Applied Nanoscience 3*, 37-40. doi:10.1007/s13204-012-0072-1

Filali, B.E., Torchynska, T. V. Díaz-Cano, A. I., Morales Rodriguez M. (2015). Structural and Raman scattering studies of ZnO Cu nanocrystals grown by spray pyrolysis. *Revista Mexicana de Ingeniería Química 14*, 781-788.

Flickyngerová, S., Tvarožek, V. and Găspierik, P. (2010). Zinc oxide - a unique material for advanced photovoltaic solar cells. *Journal of Electrical Engineering 61*, 291-295. doi:10.2478/v10187-010-0043-2

Ghosh, M., Kurian, M., Veerender, P., Padma, N., Aswal, D. K., Gupta, S. K. and Yakhmi, J. V. (2013). Photovoltaic properties of ZnO nanoparticle based solid polymeric photoelectrochemical cells. *AIP Conference Procedings 1313*, 394-396. doi:10.1063/1.3530557

Ghosh, T., Das, A. B., Jena, B. and Pradhan, C. (2015). Antimicrobial effect of silver zinc oxide (Ag-ZnO) nanocomposite particles. *Frontiers in Life Science 8*, 47-54. doi:10.1080/21553769.2014.952048

Gullapalli, H., Vemuru, V. S. M., Kumar, A., Botello-Mendez, A., Vajtai, R., Terrones, M., Nagarajaiah, S. and Ajayan, P. M. (2010). Flexible piezoelectric ZnO-paper nanocomposite strain sensor. *Nano Micro Small 6*, 1641-1646. doi:10.1002/smll.201000254

Gusatti, M., Barroso, G. S., Maduro de Campos, C. E., Ribeiro de Souza, D. A., de Almeida do Rosário, J., Bohn Lima, R., Cardoso Milioli, C., Abreu Silva, L., Gracher Riella H. and

Cabral Kuhnen, N. (2011). Effect of different precursors in the chemical synthesis of ZnO nanocrystals. *Materials Research 4*, 264-267. doi:10.1590/S1516-14392011005000035

Gusatti, M., Campos, C. E., Sousa, D. A., Moser, V. M., Kuhnen, N. C. and Riella, H. G. (2013). Effect of reaction parameters on the formation and properties of ZnO nanocrystals synthesized via a rapid solochemical processing. *Journal of Nanoscience and Nanotechnology 13*, 8303-8314. doi: 10.1166/jnn.2013.7924

Gusatti, M., do Rosário, J. A., de Campos, C. E., Kunhen, N. C., de Carvalho, E. U., Riella, H. G. and Bernardin, A. M. (2010). Production and characterization of ZnO nanocrystals obtained by solochemical processing at different temperatures. *Journal of Nanoscience and Nanotechnology 10*, 4348-4351. doi:10.1166/jnn.2010.2198

Hingorani, S., Pillai, V., Kumar, P., Multani, M. S. and Shah, D. O. (1993). Microemulsion mediated synthesis of zinc-oxide nanoparticles for varistor studies. *Materials Research Bulletin 28*, 1303-1310. doi:10.1016/0025-5408(93)90178-G

Ibrahem, E. J., Thalij, K. M., Saleh, M. K. and Badawy, A. S. (2017). Biosynthesis of zinc oxide nanoparticles and assay of antibacterial activity. *American Journal of Biochemistry and Biotechnology 13*, 63-69. doi: 10.3844/ajbbsp.2017.63.69

Kalyamwar, V. S., Raghuwanshi, F. C., Jadhao, N. L. and Gadewar, A. J. (2013). Zinc oxide nanostructure thick films as H_2S gas sensors at room temperature. *Journal of Sensor Technology 3*, 31-35. doi: 10.4236/jst.2013.33006

Kong, X. Hu, Y. and Pan, W. (2017). Controllable preparation and photocatalytic activity of highly ordered ZnO nanoarrays. *Micro & Nano Letters 12*, 461-465. doi: 10.1049/mnl.2016.0819

Lim, B. P., Wang, J., Ng, S. C., Chew, C. H. and Gan, L. M. (1998). A bicontinuous microemulsion route to zinc oxide powder. *Ceramics International 24*, 205-209. doi:10.1016/S0272-8842(97)00003-5

Lin, J. C., Lee, C. P., and Ho, K. C. (2012). Zinc oxide synthesis via a microemulsion technique: morphology control with application to dye-sensitized solar cells. *Journal of Materials Chemistry 22*, 1270-1273. doi: 10.1039/C1JM15227K

Lupan, O., Pauporte, T. and Chow, L. (2014). Synthesis and gas sensor applications of nanostructured ZnO grown at low temperatures. *Turkish Journal of Physics 38*, 399-419. doi: 10.3906/fiz-1406-21

Montgomery, D. C. (2017). *Design and Analysis of Experiments*. John Wiley & Sons, United States.

Mostafa, A.A., Sayed, S.R.M., Solkamy, E.N., Khan, M., Saik, M.R., Al-Warthan, A. and Adil, S.F. (2015). Evaluation of biological activities of chemically synthesize silver nanoparticles. *Journal of Nanomaterials 2015*, 1-7. doi: 10.1155/2015/789178

Onwudiwe, D.C., Artin, T. and Strydom, C.A. (2015). Surfactant mediated synthesis of ZnO nanospheres at elevated temperature, and their dielectric properties. *Superlattices and Microstructures 2015*, 215-225. doi:10.1016/j.spmi.2015.02.003.

Ovando-Medina, V. M., Farías-Cepeda, L., Pérez-Aguilar, N. V., Rivera de la Rosa, J., Martínez-Gutiérrez, H., Romero Galarza, A., Cervantes-González, E., and Cayetano-Castro, N. (2018). Facile Synthesis of Low Band Gap ZnO Microstructures. *Revista Mexicana de Ingeniería Química 17*, 455-462. doi:10.24275/10.24275/uam/izt/dcbi/revmexingquim/2018v17n2/Ovando

Pérez-Sicairos, S., Miranda-Ibarra, S.A., Lin- Ho, S. W., Álvarez-Sánchez, J., Pérez-Reyes, J. C., Corrales-López, K. A., Morales-Cuevas, J. B. (2016). Membranas de nanofiltración, preparadas vía polimerización en interfase, dopadas con nanopartículas de ZnO: efecto en su desempeño. *Revista Mexicana de Ingeniería Química 15*, 961-975.

Pookmanee, P., Attaveerapat, I., Kittikul, J. and Phanichphant, S. (2010). Effect of pH on zinc oxide powder prepared by a chemical coprecipitation method effect. *Advances Materials Research 93-94*, 691-694. doi: 10.4028/www.scientific.net/AMR.93-94.691

Reshak, A.H., Yanchuk, O. M., Prots, D. I., Tsurkova, L. V., Marchuk, O. V., Urubkov, I. V., Pekhnyo, V. A., Fedorchuk, O., Alahmed, Z. A. and Kamarudin, H. (2014). Optically stimulated piezoelectric effects in the electrochemically synthesized ZnO nanoparticles. *International Journal of Electrochemical Science 9*, 6378-6386.

Romo, L.E., Saade, H., Puente, B., López, M. L., Betancourt, R. and López, R. G. (2011). Precipitation of zinc oxide nanoparticles in bicontinuous microemulsions. *Journal of Nanomaterials 2011*, 1-9. doi:10.1155/2011/145963

Sharma, J., Vashishtha, M. and Shah, D. O. (2014). Crystallite size dependence on structural parameters and photocatalytic activity of microemulsion mediated synthesized ZnO nanoparticles annealed at different temperatures. *Global Journal of Science Frontier Research: B Chemistry 14*, 19-31.

Shim, J. B., Grant, J. W., Harrell, W.R., Chang, H. and Kim, S. (2011). Electrical properties of rapid hydrothermal synthesised Al-doped zinc oxide nanowires in flexible electronics. *Micro & Nano Letters 6*, 147-149. doi: 10.1049/mnl.2010.0226

Shymaa, S. A. and Asmaa, S. (2014). Synthesis and characterization of ZnO nano-rods at different temperature. *International Journal of Application or Innovation in Engineering & Management 3*, 57-62.

Sornalatha, D. J., Bhuvaneswari, S. Murugesanc, S. and Murugakoothan, P. (2015). Solochemical synthesis and characterization of ZnO nanostructures with different morphologies and their antibacterial activity. *International Journal for Light and Electron Optics 126*, 63-67. doi: 10.1016/j.ijleo.2014.07.138

Swaroop, K. and Somashekarappa, H. M. (2015). Effect of pH values on surface morphology and particle size variation in ZnO nanoparticles synthesised by co-precipitation method. *Research Journal of Recent Sciences 4*, 197-201.

Wasan, R. S., Nada M. S., Wesam, A. T. and Mohammed A. (2012). Synthesis sol-gel derived highly transparent ZnO thin films for optoelectronic applications. *Advances in Materials Physics and Chemistry 2*, 11-16. doi:10.4236/ampc.2012.21002

Zhang, C., Zhang, F., Xia, T., Kumar, N., Hahm, J., Liu, J., Wang, Z. L. and Xu, J. (2009). Low-threshold two-photon pumped ZnO nanowire lasers. *Optics Express 17*, 7893-7900. doi:10.1364/OE.17.007893